Using Selected Combining Algorithm for Blood Pressure Measurement in Micro MW-PPG Sensor

Wu, Chien-Ta, Department of Electrical Engineering, National Taipei University of Technology.

Wang, Ta-Wei, Department of Electrical Engineering, National Taipei University of Technology.

Chang, Cheng-Chun, Associate Professor, Department of Electrical Engineering, National Taipei University of Technology.

***Abstract*—With the rapid development of medical technology and the effects of aging, the issues related to medical care and long-term care have become extremely important. Among much physiological information, blood pressure is one of the important factors, while traditional medical instruments for blood pressure measurements are usually not portable. In this paper, the developed multi-wavelength PPG (MW-PPG) measurement module is used to collect multi-wavelength PPG signals. Three light sources with spectra range in red, green and infrared-red are used to collect15 MW-PPG signals. A Signal-to-Noise Ratio based (SNR-based) selected combining algorithm is proposed to select the PPG signal with the best signal quality. The selected MW-PPG signals with the corresponding neural network model are used for blood pressure prediction.**

In this paper, we show that based on the proposed SNR-selected combining algorithm to select the PPG wavelength for blood pressure measurement on different objects, compared to using the green PPG signal, averagely 5% MAE can be reduced in diastolic and systolic blood pressure measurement. Further, a clinical trial was conducted on 10 subjects. The results of the clinical trial show that the SNR-based selected combining algorithm could reduce the prediction error by up to 12% compared to the single wavelength PPG sensing methodology.

***Index Terms*— blood pressure prediction, multi-wavelength PPG technique, machine learning, transfer learning.**

I. INTRODUCTION

THANKS to the rapid development of embedded systems, big data analysis, and artificial intelligence in recent years, modern medicine is gradually moving towards to precision medicine. Various physiological signals such as heart rate, blood pressure, and blood sugar are continuously monitored through the wearable devices and collected into a huge database in order to build a medical big data system. Further, by using of the artificial intelligence and machine learning algorithms, the prediction model can be trained and it can be assumed as the beginning of preventive healthcare. In response to the recent COVID-19 outbreak, the healthcare metrics measured from the personalized smart wearable devices are considered as the indicators of COVID-19 infection and assessment. Since the COVID-19 virus affects the sensitivity of the nervous system to oxygen, the brain is unable to detect hypoxia in real-time, resulting in invisible hypoxia (Happy hypoxia) [1], causing medical treatment to be delayed and the golden period of treatment to be missed. The wearable device can monitor patients' blood oxygen levels in real-time and provide appropriate medical measures to reduce the mortality caused by COVID-19.

Photoplethysmography (PPG) has been widely used in wearable devices as a convenient method for heart rhythm and blood oxygen measurement. In recent years, the miniaturization of electronic components and the rapid development of PPG sensing modules have significantly contributed to the development of PPG applications for blood pressure measurement. Traditionally, many studies have pointed out that the distance between the PPG sensing signal and the peak of the ECG can be assumed as the pulse transit time (PTT). Since the PTT has a linear relationship with blood pressure, it is believed that the PTT can further infer the blood pressure value. However, the number of features is too small and the measurement needs to be used in conjunction with a large ECG measurement device, which hinders the accuracy of blood pressure prediction and makes it inconvenient to carry around to achieve portable monitoring. In 2005, Nitzan

Corresponding author: C.-C., Chang. ccchang@mail.ntut.edu.tw

The next few paragraphs should contain the authors' current affiliations, including current address and e-mail. For example, First A. Author is with the National Institute of Standards and Technology, Boulder, CO 80305 USA (e-mail: author@ boulder.nist.gov).

Second B. Author was with Rice University, Houston, TX 77005 USA. He is now with the Department of Physics, Colorado State University, Fort Collins, CO 80523 USA (e-mail: author@lamar.colostate.edu).

Third C. Author Jr. is with the Electrical Engineering Department, University of Colorado, Boulder, CO 80309 USA, on leave from the National Research Institute for Metals, Tsukuba 305-0047, Japan (e-mail: author@nrim.go.jp).

Mentions of supplemental materials and animal/human rights statements can be included here.

Color versions of one or more of the figures in this article are available online at http://ieeexplore.ieee.org

et al [2] show that the PPG signals from different body parts are captured and the time difference between the peaks of the PPG signals can be used as the PTT to predict blood pressure. However, the sensor must be carried on different body parts, which makes it inconvenient to carry. After 2009, many researchers [3][4] started to study the extraction of multiple features by single wavelength PPG signals for blood pressure measurement, and the amount of feature extraction has been gradually increased from 4 to 21, and the error has reached less than 4%, which innovates PPG application for blood pressure measurement.

However, many studies have pointed out that the captured PPG sensing signals is susceptible to environmental variables such as skin surface relaxation [5], skin color [6], skin surface temperature [7], etc. To obtain stable signal quality, MW-PPG sensing technology has been gradually gaining attention in recent years. Since PPG signals of different wavelengths can penetrate different skin depths [8]-[11], Zhang et al [12] pointed out in 2019 that short-wavelength PPG signals have a higher Signal to Motion Artifacts Ratio (SMR) compared to long-wavelength PPG signals. Therefore, the short wavelength PPG signal can be used as the main signal, while the long wavelength PPG signal is more sensitive to dynamic noise, so the dynamic noise can be extracted by spectrum analysis and subtracted from the main signal to eliminate the dynamic noise to obtain a more stable PPG signal. Chang et al [13] also used a micro spectrometer sensor chip to build an MW-PPG measurement device in 2019. The developed signal processing algorithm can extract robust heart rhythm and blood oxygen detection values, and further, validate the feasibility of MW-PPG for blood pressure sensing. In 2020 [14], they further validated that PPG signals of different wavelengths in different postures can provide different signal-to-noise ratios (SNR), and the signal combining algorithm allows the wearer to merge PPG signals with high SNR from MW-PPG sensors in different postures. On average, the PPG signal has a 28% higher SNR than conventional single wavelength PPG signals in different postures.

The MW-PPG measurement module which had been established in our past studies [13] was continually adopted in this paper to collect MW-PPG signals and explore the selection of PPG signal bands for different subjects by selected combining algorithm to achieve blood pressure measurement via neural network. In terms of neural network training in this paper, the transfer learning algorithm is used due to the difficulty of medical data is collection. Based on the transfer learning, the experience, knowledge, and features learned from the neural network trained by the source dataset can be transferred to the model for the target dataset. In our study, the publicly available MW-PPG signals database, MIMIC-III Waveform Database, is used as the source dataset to train the neural network model in advance and then transferred to the model for target dataset which is collected by the developed MW-PPG measurement module.

II. Background Knowledge

Section 2.1 introduce the the module architecture and principles of the developed MW-PPG measurement module introduces, Section 2.2 introduces various feature extraction methods for blood pressure prediction, and Section 2.3 introduce the neural networks and transfer learning development in the AI field.

A. Micro MW-PPG Measurement Module

The MW-PPG measurement module used in this paper is shown in Figure 1(a). The light sources are arranged symmetrically, and the MW-PPG sensor is placed in the middle, so that the light sources of different wavelengths can be reflected by the skin and gathered at the center to facilitate the collection of MW-PPG sensors. Three sets of LEDs are used for the light source, which are green light (wavelength 515 nm), red light (wavelength 660 nm), and infrared light (wavelength 940 nm), and the spectra of the three light sources are shown in Figure 1(b). The nanoLambda micro spectrometer is used as the receiver side sensor for MW-PPG signal detection. Compared with conventional spectrometers, which are often several square centimeters, this sensor only occupies a few square microns. Since it does not use precision optical components such as grating and focal lens, it is small and light in use and can collect 15 wavelengths of PPG signals including 505nm, 510nm, 515nm, 520nm, 525nm, 620nm, 625nm, 630nm, 635nm, 640nm, 930nm, 935nm, 940nm, 945nm, and 950nm at the same time. Also, compared to conventional Photo-diodes (PDs) that obtain PPG signals of different wavelengths by time-sharing and multiplexing through SWITCH, and then recombine these fragmented signals into multi-wavelength PPG signals, the MW-PPG measurement module used in this paper can simultaneously resolve PPG signals of multiple wavelengths, and the signals do not need to go through the recombination process, such that we can have true real-time MW-PPG signals. According to a previous study [13], this measurement module can achieve the advantage of simultaneous and robust measurement compared with the conventional PD.

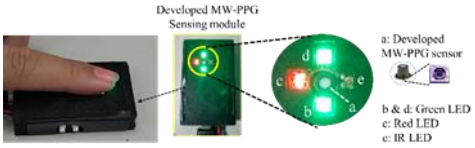

(a) NSP32 multi-wavelength PPG measurement module

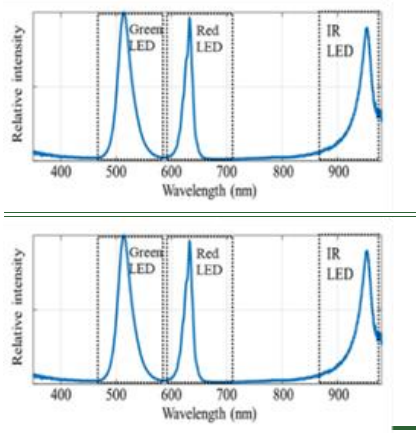

(b) The spectra of the three light sources

Fig. 1. Pictorial and used spectra of the light source in the MW-PPG measurement module

The mathematical model of the MW-PPG sensing device in this study is shown in Figure 2. The PPG sensor signal at each wavelength captured by the micro MW-PPG sensor can be expressed as

$$\mathbf{y}_t = \mathbf{F}_t \mathbf{x}_t^T + \mathbf{n}_t , \quad (1)$$

where $\boldsymbol{y}_t = [y_{1,t} \quad y_{2,t} \quad , \copyright, \quad y_{L,t}]$, and $y_{i,t}, i \copyright \ldots, L$ is the PPG sensing signal collected at time t for the i-th wavelength, $\boldsymbol{F} = [\boldsymbol{f}_1^T \quad \copyright \quad , \ldots, \quad \boldsymbol{f}_L^T]$, where $\mathbf{f}_i^T, i = 1, \ldots, L$ is the response curve of the i-th sensing wavelength. In this study, we assume that the response curve of a sensing wavelength is an approximately perfect Gaussian curve, $\mathbf{x}_t$ is the reflected spectrum received by the sensor, and $\mathbf{n}_t$ is the noise component of the received signal.

From [15], the PPG sensing signal at each wavelength can be divided into the signal $\mathbf{x}$ (freq.<7 Hz) and noise $\mathbf{n}$ (freq.>7 Hz) components. The signal component is used for the feature extraction and model training, and the signal and noise components are used to calculate the SNR values, which are used to evaluate the signal selection at each wavelength.

$$\mathbf{y}_t = \mathbf{s}_t + \mathbf{n}_t , \quad (2)$$

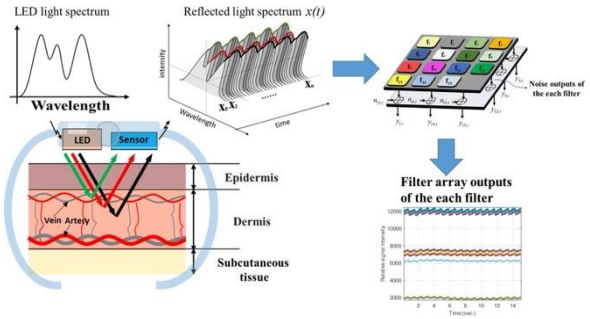

Fig. 2. Mathematical model of MW-PPG sensing device

B. PPG Blood Pressure Feature Extraction

The association between PPG signals and blood pressure has been studied in the past, and PPG signals can record the pulsatile changes in blood flow in subcutaneous vessels during each heartbeats. The changes in the waveform would be related to cardiac blood transfusion, vessel shape, and vessel wall condition. Therefore, many studies have been conducted to predict blood pressure by means of analyzing the features of the PPG waveform in various ways.

In the frequency domain, Xing et al [16] used the data in MIMIC II to extract the amplitude and phase in the waveform by FFT transformation. They concluded that this method is more stable than extracting features from the time domain because there is no need to capture the location of particular time points, and multiple periodic pulse signals can be analyzed at one time. Subsequently, the Levenberg-Marquardt algorithm in ANN was used to train the amplitude and phase as features, and the final predicted results were -1.67 ± 2.46 mmHg for SBP and -1.29 ± 1.71 mmHg for DBP.

In the time domain, as shown in figure 3, Suzuki et al [3] calculated the turning points on a single PPG waveform by quadratic differentiation and recorded the four main turning points PW, TW, Dn, and DW on the PPG waveform as characteristic parameters and predicted the SBP values by the Error-Correcting Output Codes (ECOC) method. The predicted results were r=0.75, MD=-1.2 [mmHg], and SD=11.7 [mmHg]. In addition, Kurylyak et al [4] concluded that the feature point of the PPG waveform is the time difference between peak and trough in a single pulse, and the time difference at each pulse height is considered as the variation of blood flow with the pulsation of the heart, and based on the characteristics adopted in other previous papers: the horizontal distance of the pulse at pulse heights of 10% [17], 50% and 66% [18]. To fully express the pulse information, 25%, 33%, and 75% were added as feature parameters. In this study, 21 features extracted from a single PPG waveform are used as input to the neural network model, and the MIMIC database data was used for training data. As a results, absolute error 3.80±3.46(mmHg) and 2.21±2.09(mmHg) for SBP and DBP can be achieved

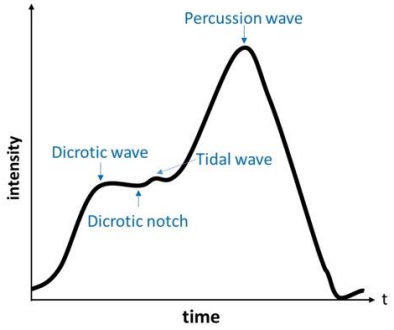

Fig. 3. Basic feature of PPG signal in time-domain

C. Neural Networks And Transfer Learning

With the development of technology, AI have been gaining attention from the public, among which Artificial Neural Network (ANN) is a mathematical model that imitates the structure and function of the human brain, being used to perform regression and classification. The number of neuron features that can be trained increases as the computing speed and performance of the graphics chip increase, allowing the neural network model to achieve better learning results.

The amount of training data is always the key to deciding whether a model is good or bad, but not all data acquisition methods are simple. Especially in the medical field, it is not easy to collect each piece of data. To solve these problems, some researchers have developed transfer learning methods as shown in Figure 4. Transfer learning is a special area of research in machine learning, and its research is based on the idea so that when humans encounter a new problem, they can solve the new problem faster and more efficiently based on their previous experience and knowledge, which is a process of transferring knowledge. Therefore, as long as a model with the same or related task as the neural network model to be trained can be found, it can be used as the source domain model and the target domain model can be trained by transfer learning, instead of collecting enough data, labeling data and training the model on

the target domain from scratch, which greatly saves the time of data collection.

In this paper, due to the limited amount of data that can be collected using the MW-PPG sensor, the results of neural network model training are usually unsatisfactory, so the MIMIC public database data are used as the training data to train neural network with source domain knowledge. The source domain neural network model is used as the initial model to train with the collected data from the MW-PPG sensor.

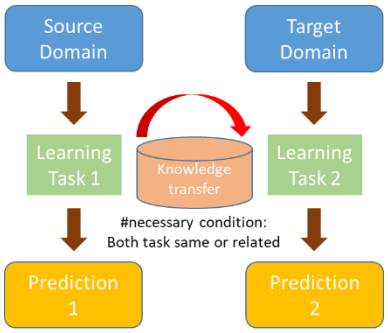

Fig. 4. Transfer learning method

III. Proposed Algorithm for MW-PPG Blood Pressure Measurement

A. Pre-processing of the Signal

Before the feature capture, there are many noises generated in the circuit operation such as thermal noise, white noise, shot noise, etc. Generally, the frequency of heartbeat is between 60 and 100 (bpm), so it can be seen that the frequency range of the PPG signal is about 0.5~7Hz [15], as shown in Figure 5. To obtain the PPG sensing signal without noise, the raw PPG sensing signal y at time t is filtered by a bandpass filter to remove the high and low-frequency noise (Fstop1:0.1708 Hz, Fstop2:6 Hz, Fpass1:0.9 Hz, Fpass2:7 Hz). The raw PPG sensing signal passed with a bandpass filter can be expressed as $\tilde{y}_{i,t}$.

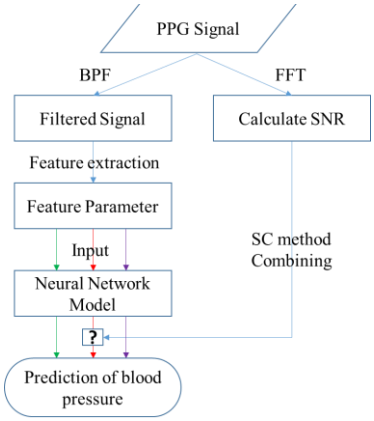

Fig. 5. Data pre-processing method

Next, the feature extraction technique in Section 2.2 is used to extract 21 feature parameters from the noise-filtered PPG sensing signal, including CP (Cardiac Period), SUT (Systolic upstroke Time), DT (Diastolic Time), 6 parameters of DW (Diastolic Width), 6 parameters of SW (Systolic Width) + DW, and 6 parameters of DW/SW, as shown in Figure 6. In addition, we further extend the method by including the 6 SW values as feature parameters for training.

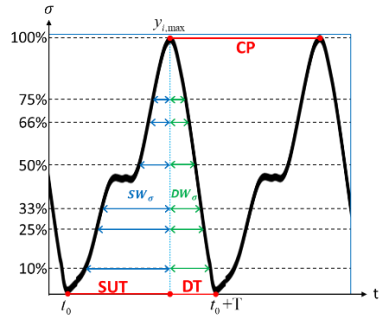

Fig. 6. PPG signal feature extraction

Since [4] holds that the feature point of the PPG waveform is the time difference between the peak and the trough in a single pulse, the time difference under each pulse height σ emerges as the change of blood flow with the heartbeat. In this study, according to [4], the reference points of the PPG waveform are used as feature parameters, where each feature parameter is calculated by the following mathematical equations.

Following equation (2) and (3), a single pulse of PPG signal can be expressed as

$$\boxed{\tilde{y}_{i,t_0 \to t_0+T}} \text{ (miss i)}, \tag{4}$$

where t_0 is the start time of a single pulse, T is the period of the PPG signal. In the *i*-th wavelength signal, the peak value $y_{i,\max}$ of the single pulse and the peak time point $t_{i,\max}$ can be expressed as

$$\begin{cases} y_{i,\max} = \max\limits_{t\in[t_0,t_0+T]} \tilde{y}_{i,t} \\ t_{i,\max} = \arg\max\limits_{t\in[t_0,t_0+T]} \tilde{y}_{i,t} \end{cases}, \tag{5}$$

The time differences from peak to trough SUT and DT, and the time difference from the peak of a pulse wave to the peak of the pulse wave in the next cycle CP can be expressed as

$$\begin{cases} SUT = t_{i,\max} - t_0 \\ DT = (t_0 + T) - t_{i,\max} \\ CP = t_{i,\max}(T+1) - t_{i,\max}(T) \end{cases}, \tag{6}$$

In addition, SW_σ and DW_σ are the peak height of the pulse at each ratio σ. The time difference from the peak can be expressed as

$$\begin{cases} \mathrm{SW}_\sigma = t_{i,\max} - t_{start,\sigma} \\ \mathrm{DW}_\sigma = t_{end,\sigma} - t_{i,\max} \end{cases}, \tag{7}$$

where $t_{start,\sigma}$ and $t_{end,\sigma}$ are the time points closest to the value of y_σ in the left and right sides of the wave peak.

$$\begin{cases} t_{start,\sigma} = \arg \min\limits_{\substack{t\in[t_0,t_0+T] \\ t\le t_{i,\max}}} \left| y_{i,t} - y_\sigma \right| \\ t_{end,\sigma} = \arg \min\limits_{\substack{t\in[t_0,t_0+T] \\ t\ge t_{i,\max}}} \left| y_{i,t} - y_\sigma \right| \end{cases}, \quad (8)$$

and y_σ is the peak height of the pulse at different ratios of σ

$$\begin{cases} y_\sigma = \sigma \cdot y_{i,\max} \\ \sigma = 0.1, 0.25, 0.33, 0.5, 0.66, 0.75 \end{cases}, \quad (9)$$

As a result, the 27 features ε can be extracted from Eqs. (4) to (9).

$$\varepsilon = [\mathrm{CP}, \mathrm{SUT}, \mathrm{DT}, \mathrm{SW}\sigma, \mathrm{DW}\sigma, \mathrm{SW}\sigma + \mathrm{DW}\sigma, \mathrm{DW}\sigma / \mathrm{SW}\sigma]$$

B. Neural Network Model Training

The 27 features are used as the input to the neural network model. In this neural network model framework, the mean square error (MSE) is used for the loss function, Adam is used for the optimizer, and a multilayer perceptron (MLP) framework with 6 hidden layers is used for training. In addition, for the target domain neural network model, the data augmentation method is used to avoid the lack of data in the target domain and the excessive computation caused by training 15 different wavelengths of neural network models. The sensor uses three types of LED light sources: green, red, and infrared, each of which captures five PPG signals of similar wavelengths as the same set of target domain data. The green wavelength bands 505nm, 510nm, 515nm, 520nm, and 525nm are considered the same group. The red wavelengths 620nm, 625nm, 630nm, 635nm, and 640nm are considered the same group. Infrared wavelengths 930nm, 935nm, 940nm, 945nm, and 950nm are considered the same group. The parameters of Layers 1 and 2 are retrained, and the parameters of other layers are fixed. And then the data measured in the MIMIC database are transferred to the three separate green, red, and infrared target field neural network models using the layer transfer method.

C. SNR-based Selected combining Algorithm

In this study, the PPG signal wavelength with the best signal-to-noise ratio (SNR) is selected as the wavelength band for blood pressure prediction by a selected combining algorithm. Since the selected combining algorithm has been widely used in the field of MIMO communication, this study applies this theory to select three types of green, red, and infrared neural network models. In this study, the SNR is calculated as follows: after converting the time domain signal to the frequency domain signal, the normal PPG signal frequency is 0.5Hz~7Hz, where freq.<7 Hz is defined as signal and freq.>7 Hz is defined as noise, and the SNR is calculated by dividing the signal power by the noise power. The strength of SNR means the stability of the waveform in the PPG signal, and the selection of the PPG signal wavelength with the best SNR means that the PPG signal with better signal quality can be used for prediction.

Through the selected combining algorithm, the predicted blood pressure values of each wavelength can be merged into one predicted blood pressure value by the algorithm, and the mathematical equation can be expressed as

$$SCmethod(SBP, DBP) = \sum_{i=1\ldots L} \omega_i (\mathrm{SBP_i}, \mathrm{DBP_i}), \quad (10)$$

$$\omega_i = \begin{cases} 1, snr_i = \max\limits_{i=1\ldots M}(snr_i) \\ 0, otherwise \end{cases}, \quad (11)$$

where ω_i is the weight of the *i*-th wavelength, SNR is the signal-to-noise ratio, and the mathematical equation can be expressed as

$$\mathrm{snr_i} = \frac{\mathrm{E[s_i^2(t)]}}{\mathrm{E[n_i^2(t)]}} = \frac{\sum\limits_{f\le 7Hz} \tilde{s}_i^{\,2}(f)}{\sum\limits_{f>7Hz} \tilde{n}_i^{\,2}(f)}, \quad (12)$$

As shown in Figure 7, a 20-second MW-PPG sensing signal was collected, and the SNRs of red, green, and infrared light were 31.52(dB), 18.90(dB), and 26.57(dB), respectively. In addition, Figure 7(b) shows that the waveform of the red PPG sensor signal is clearer than those of the green and infrared signals. Given this, the SNR-based selected combining algorithm was used to select the blood pressure prediction results of the red PPG signal with better SNR. Besides, the mean absolute error (MAE) of the red PPG signal was 5.18 (mmHg). Furthermore, the prediction errors of green and infrared light were MAE 15.25(mmHg) and MAE 8.47(mmHg), respectively, which further verified that the signal quality and the prediction error of blood pressure were positively correlated.

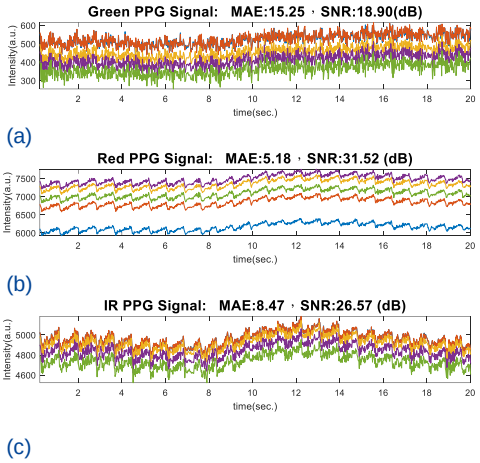

Fig. 7. A set of 20-second measurement signals of the micro MW-PPG measurement module, where (a) is the measurement signal with a wavelength from 505 nm to 525 nm, (b) is the measurement signal with a wavelength from 620 nm to 640 nm, and (c) is the measurement signal with a wavelength from 930 nm to 950 nm.

IV. Experimental Results

A. Experimental Data Collection and Test Results

In this study, the micro multi-wavelength MW-PPG blood pressure monitor introduced in Section 2 is used for research sampling and data collection with 89 MW-PPG signals collected, and each MW-PPG signal contains 15 bands, including red band (505, 510, 515, 520, 525 nm), green band (620, 625, 630, 635, 640 nm), and infrared band (940, 945, 950, 955, 960 nm). Given the difficulty of data collection for human experiments, five close wavelengths of the same light source are used to train the blood pressure measurement model for that color to realize the increase in the amount of data collection through the expansion of the data. In addition, each MW-PPG sensing signal is collected for 20 seconds for signal-to-noise ratio analysis. During the collection process, a commercially available cuff blood pressure monitor (OMRON HEM-7121) is used to measure the diastolic and systolic blood pressures of the subjects as ground truth. The systolic blood pressure range of the subjects in this study is 63-88 mmHg, and the diastolic blood pressure is 81-133 mmHg.

The architecture of the blood pressure measurement model for each wavelength is shown in the following table. In order to avoid overfitting due to the small data set collected, migration learning was used to train the original model using a total of 12,500 data from the public database (MIMIC III), as shown in Table 1. Then, Layer 6 and the output layer were used as the migration layer. The target model was trained with 70%, 15%, and 15% of the collected data as training data, validation data, and test data for micro multi-wavelength blood pressure monitors.

TABLE I
SW PPG BP ARCHITECTURE FOR EACH RED, GREEN, AND INFRARED PPG SIGNALS

Layer	Operator
1	FC 27x256 + ReLU
2	FC 256x256 + ReLU
3	FC 256x256 + ReLU
4	FC 256x256 + ReLU
5	FC 256x128 + ReLU
6	FC 128x64 + ReLU
7	FC 64x2

For the data testing, 89 data were collected and tested. Figure 8 shows the mean absolute errors of the systolic and diastolic pressure measurements in different ways for each test data. The red, green, and blue lines are the measured MAE of the blood pressure when using red, green, and infrared red PPG signals, respectively, and the black line is the MAE when the PPG signal selected according to the proposed SNR of -based selective combining algorithm. It is worth noting that the wavelength of the minimum MAE varies from measurement data to measurement data, which is explained in Section 1. Therefore, the wavelength of PPG signal with optimal SNR also varies for different measurements. In terms of systolic pressure, the MAE was 6.7(mmHg), 7.2(mmHg), and 6.47(mmHg) for red, green, and infrared light, respectively. If the light source with the lowest MAE is selected for each measurement, the average MAE can reach 5.1(mmHg). On the other hand, 6.13(mmHg) MAE can be achieved by using the selected combining algorithm proposed in this study, which can reduce the error by 9.2%, 17.4%, and 5.5% compared to green light, infrared light, and red light, respectively. Furthermore, for diastolic blood pressure, the MAE 4.79(mmHg), 4.98(mmHg), and 4.54(mmHg) for the infrared, green, and red lights are achieved, respectively. If the light source with the lowest MAE is selected for each measurement, the average MAE can reach 3.61(mmHg). Compared to that, the 4.53(mmHg) MAE can be achieved by using the selected combnining algorithm proposed in this study, which can reduce the error by 5.7%, 9.9%, and 0.2% compared to green, red, and infrared lights respectively. It can be seen that although the selected combining algorithm can not always select the wavelength with lowest MAE, while based on the SNR as reference, we can dynamically select the wavelength for blood pressure measurement which is not the worst. As a result, compared to using the green PPG signal for the blood pressure measurements, the averaged MAE of systolic and diastolic pressures can be reduced up to 5% when the proposed SNR-based selected combining algorithm is used

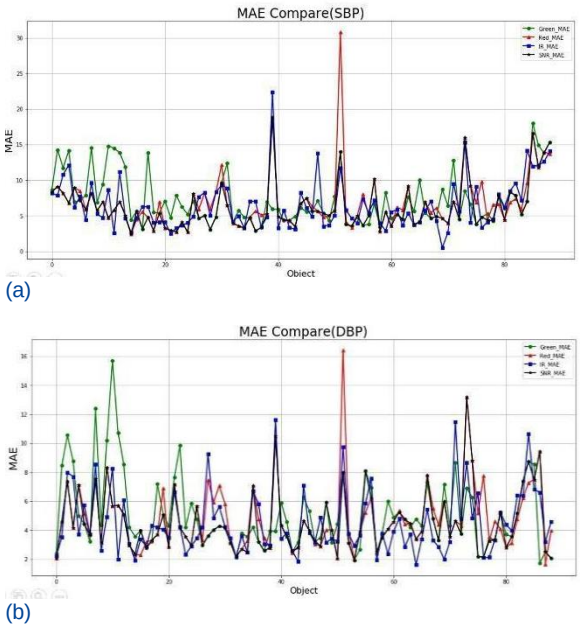

Fig. 8. MAE of (a) SBP and (b) DBP for 89 measurements with the use of red, green, and IR lights and the proposed SNR-based selected merged PPG signals.

B. Clinical Test Results

In this study, the developed micro MW-PPG sensing device was further tested on ten subjects in the clinical setting, as shown in Figure 9, where (a) and (b) show the systolic and diastolic MAE respectively measured by different light sources in the micro MW-PPG sensing device for the ten subjects. The red, green, blue, and black lines are the results of the MW-PPG sensing device using red, green, infrared, and SNR-based algorithms, respectively. It is noteworthy that the MAE of systolic and diastolic pressures are different for the same light source in the same subject. For example, the diastolic MAE of Subject 5 was 2.59(mmHg), 3.59(mmHg), and 4.73(mmHg) under red, green, and infrared light, respectively, and the systolic MAE was 6.71(mmHg), 5.85(mmHg), and 6.96(mmHg) under red, green, and infrared light, respectively. The MAE of

red light was found to be the best in diastolic blood pressure, better than green light at 1 (mmHg) and infrared light at 2.14 (mmHg), while the MAE of green light was the best in diastolic blood pressure, better than red light at 0.86 (mmHg) and infrared light at 1.11 (mmHg). If the green light is selected for blood pressure measurement, although more accurate results can be obtained for diastolic blood pressure, there is a loss of 1(mmHg) in accuracy for systolic blood pressure compared to red light in MAE. In contrast, if the red light is selected for blood pressure measurement, although the lowest measurement error is obtained in systolic pressure, there is a loss in accuracy of 0.86(mmHg) in diastolic pressure compared to green light in MAE. Therefore, as described in Section 1 of this paper, due to the differences in the nature of the skin of different subjects and various environmental variables, the light source suitable for systolic and diastolic blood pressure measurements will change accordingly. Therefore, the selection of an appropriate light source for blood pressure measurement is a major challenge for different subjects.

Compared with the measurement method using only a single light source, the SNR-based selected combining algorithm proposed in this paper can select the best results in terms of the average MAE of systolic and diastolic pressures among different subjects. For example, for Subject 5, the average MAE of the red light source selected by the SNR-based selected combining algorithm was better than that of the green light (4.72 mmHg) and infrared light (5.85 mmHg). In addition, among all 10 subjects, the results of the proposed selected combining algorithm were used to select the lowest average MAE for 5 subjects and the next best average MAE for the remaining 5 subjects. The SNR-based selected combining algorithm by signal quality profiling does not guarantee the selection of the source with the lowest average MAE, but it can relatively select the source with 50% of the best and 50% of the second best MAE.

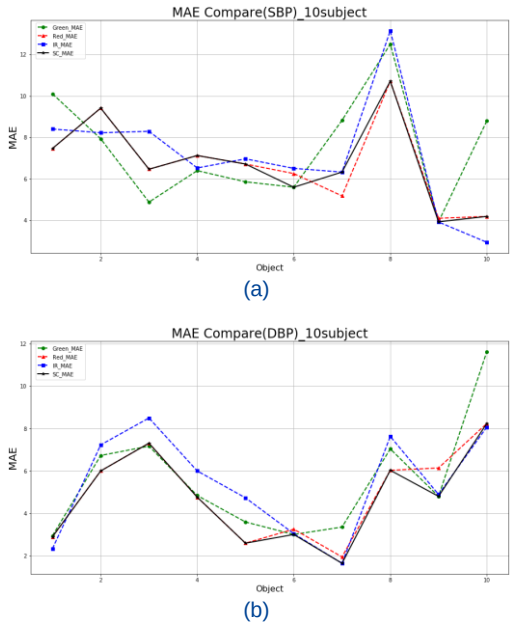

Fig. 9. MAE of (a) SBP and (b) DBP for 10 clinical test measurements with the use of red, green, and IR lights and the proposed SNR-based selected merged PPG signals.

V. Conclusions

In this study, based on the micro MW-PPG measurement module developed in [13], 15 sets of wavelengths of MW-PPG signals were collected from three light sources, and the blood pressure measurement models were trained under each light source by transfer learning and deep learning algorithms. The SNR-based selected combining algorithm was used to select the light source with the best signal quality and to predict blood pressure by the corresponding neural network model. This method achieves an average error improvement of up to 5% in diastolic blood pressure. In addition to the training dataset and the test dataset, ten clinical tests were also collected to determine the quality of blood pressure. The average MAE of green, infrared, and red light was 5.75(mmHg), 6.09(mmHg), and 5.51(mmHg), respectively, and the SNR-based selected combining algorithm was further validated to reduce the prediction error through clinical testing. The MAE can reach 5.33(mmHg) if the selected combining algorithm proposed in this paper is used, which can reduce the error by up to 12% compared to the single light source.

All experiments and data collection were performed under the supervision of the Chang Gung Medical Foundation Institutional Review Board.

B. Final Stage Using IEEE Author Portal

Upon acceptance, you will receive an email with specific instructions regarding the submission of your final files. Final submissions should include a nicely formatted pdf of the entire article as well as source files of your accepted manuscript, including high quality graphic files. Immediately after you have submitted your final files, you will be automatically redirected to the IEEE electronic copyright form wizard. Please complete the copyright at that time to avoid publication delays. If you have any questions regarding the final submission process, please contact the administrative contact for the journal.

VI. Conclusion

In this study, based on the micro MW-PPG measurement module developed in [13], 15 sets of wavelengths of MW-PPG signals were collected from three light sources, and the blood pressure measurement models were trained under each light source by transfer learning and deep learning algorithms. The SNR-based selected combining algorithm was used to select the light source with the best signal quality and to predict blood pressure by the corresponding neural network model. This method achieves an average error improvement of up to 5% in diastolic blood pressure. In addition to the training dataset and the test dataset, ten clinical tests were also collected to determine the quality of blood pressure. The average MAE of green, infrared, and red light was 5.75(mmHg), 6.09(mmHg), and 5.51(mmHg), respectively, and the SNR-based selected combining algorithm was further validated to reduce the prediction error through clinical testing. The MAE can reach 5.33(mmHg) if the selected combining algorithm proposed in this paper is used, which can reduce the error by up to 12% compared to the single light source.

All experiments and data collection were performed under the supervision of the Chang Gung Medical Foundation Institutional Review Board.

REFERENCES

[1] M. Uginet, G. Breville, F. Assal, K.-O. Lövblad, M. I. Vargas, J. Pugin, J. Serratrice, F. R. Herrmann, P. H. Lalive, G. Allali, "COVID-19 encephalopathy: Clinical and neurobiological features," Wiley Journal of Medical Virology, vol. 93, no. 7, pp. 4374-4381, July 2021.

[2] M. Nitzan, C. Rosenfeld, A. T. Weiss, E. Grossman, A. Patron and A. Murray, "Effects of external pressure on arteries distal to the cuff during sphygmomanometry," IEEE Transactions on Biomedical Engineering, vol. 52, no. 6, pp. 1120-1127, June 2005.

[3] S. Suzuki and K. Oguri, "Cuffless blood pressure estimation by error-correcting output coding method based on an aggregation of AdaBoost with a photoplethysmograph sensor," in proc. of 2009 Annu. Int. IEEE EMBS Conf., Minneapolis, MN, 2009.

[4] Y. Kurylyak, F. Lamonaca and D. Grimaldi, "A neural network-based method for continuous blood pressure estimation from a PPG signal," in proc. of 2013 IEEE I2MTC, Minneapolis, MN, pp. 280-283, 2013.

[5] J Liu et al. "Multi-wavelength photoplethysmography method for skin arterial pulse extraction." Biomedical optics express, vol. 7, no. 10, pp. 4313-4326, Sep. 2016.

[6] L. Yan, S. Hu, A. Alzahrani, S. Alharbi and P. Blanos, "A multi-wavelength opto-electronic patch sensor to effectively detect physiological changes against human skin types, " Biosensors, vol. 7, no. 2, pp. 1-12, June 2017.

[7] Y. Maeda, M. Sekine, T. Tamura, A. Moriya, T. Suzuki and K. Kameyama, "Comparison of reflected green light and infrared photoplethysmography", in proc. of 30th Annu. Int. IEEE EMBS Conf., pp. 2270-2272, Aug. 2008.

[8] J. Lee, K. Matsumura, K. Yamakoshi, P. Rolfe, S. Tanaka and T. Yamakoshi, "Comparison between red, green and blue light reflection photoplethysmography for heart rate monitoring during motion," the 35th Annual International Conference of the IEEE Engineering in Medicine and Biology Society (EMBC), pp. 1724-1727, Osaka, 2013.

[9] J. Spigulis, L. Gailite, R. Erts and A. Lihachev, "Contact probe pressure effects in skin multi-spectral photoplethysmography," European Conference on Biomedical Optics, pp. 307-314, Munich, 2007.

[10] L. Yan, S. Hu, A. Alzahrani, S. Alharbi and P. Blanos, "A multi-wavelength opto-electronic patch sensor to effectively detect physiological changes against human skin types," Biosensors, vol. 7, no. 2, pp. 1-12, Jun. 2017.

[11] Y. Maeda, M. Sekine, and T. Tamura, "The advantages of wearable green reflected photoplethysmography," Journal of Medical Systems, vol. 35, no. 5, pp. 829-834, Oct. 2011.

[12] Y. Zhang et al. "Motion artifact reduction for wrist-worn photoplethysmograph sensors based on different wavelengths," Sensors, vol. 19, no 3, pp.673, Feb. 2019.

[13] C. C. Chang, C. T. Wu, B. I. Choi and T. J. Fang, "MW-PPG sensor: An on-chip spectrometer approach," Sensors, vol. 19, no. 17, pp. 3698, 2019.

[14] S.-H. Chen, Y.-C. Chuang and C.-C. Chang, "Development of a Portable All-Wavelength PPG Sensing Device for Robust Adaptive-Depth Measurement: A Spectrometer Approach with a Hydrostatic Measurement Example," Sensors, vol. 20, no. 22, pp. 1-12, Nov. 2020.

[15] M. Elgendi, "C , E and D Waves Detection in the Acceleration Photoplethysmogram," Computer Methods and Programs in Biomedicine, vol. 117, no. 2, pp. 125–136, 2014.

[16] Xing, Xiaoman; Sun, Mingshan (2016). Optical blood pressure estimation with photoplethysmography and FFT-based neural networks. Biomedical Optics Express, 7(8), 3007–. doi:10.1364/BOE.7.003007

[17] S. Linder, S. Wendelken, E. Wei, and S. McGrath, "Using the morphology of photoplethysmogram peaks to detect changes in posture," Journal of Clinical Monitoring and Computing, vol.20(3), pp.151–158, June 2006.

[18] X. F. Teng and Y. T. Zhang, "Continuous and noninvasive estimation of arterial blood pressure using a photoplethysmographic approach," Proc. of 25th Annual Inter. Conf. of the IEEE Engineering in Medicine and Biology Society, Cancun, Mexico, 2003, pp. 3153 – 3156.

First A. Author (Fellow, IEEE) and all authors may include biographies if the publication allows. Biographies are often not included in conference-related papers. Please check the Information for Authors to confirm. Author photos should be current, professional images of the head and shoulders. The first paragraph may contain a place and/or date of birth (list place, then date). Next, the author's educational background is listed. The degrees should be listed with the type of degree in what field, which institution, city, state, and country, and year the degree was earned. The author's major field of study should be lowercase.

The second paragraph uses the preferred third person pronoun (he, she, they, etc.) and not the author's last name. It lists military and work experience, including summer and fellowship jobs. Job titles are capitalized. The current job must have a location; previous positions may be listed without one. Information concerning previous publications may be included. The format for listing publishers of a book within the biography is: *Title of Book* (publisher name, year) similar to a reference. Current and previous research interests end the paragraph.

The third paragraph begins with the author's preferred title and last name (e.g., Dr. Smith, Prof. Jones, Mr. Kajor, Ms. Hunter, Mx. Riley). List any memberships in professional societies other than the IEEE. Finally, list any awards and work for IEEE committees and publications.

Second B. Author photograph and biography not available at the time of publication.

Third C. Author Jr. (Member, IEEE), photograph and biography not available at the time of publication.